Brain Advance Access published May 26, 2008

doi:10.1093/brain/awn101

Central and systemic IL-1 exacerbates neurodegeneration and motor symptoms in a model of Parkinson's disease

María Clara Pott Godoy,[1,*] Rodolfo Tarelli,[1,*] Carina Cintia Ferrari,[1] Maria Inés Sarchi[2] and Fernando Juan Pitossi[1]

[1]Fundación Instituto Leloir, FBMC-UBA, CONICET, Patricias Argentinas 435. (1405) and [2]Cátedra de Matemáticas – Facultad de Farmacia y Bioquímica, Junín 954, Buenos Aires, Argentina

*These authors contributed equally to this work

Correspondence to: Fernando Pitossi, Fundación Instituto Leloir, FBMC-UBA, CONICET, Patricias Argentinas 435, (1405) Buenos Aires, Argentina
E-mail: fpitossi@leloir.org.ar

Parkinson's disease is a neurodegenerative disorder with uncertain aetiology and ill-defined pathophysiology. Activated microglial cells in the substantia nigra (SN) are found in all animal models of Parkinson's disease and patients with the illness. Microglia may, however, have detrimental and protective functions in this disease. In this study, we tested the hypothesis that a sub-toxic dose of an inflammogen (lipopolysaccharide) can shift microglia to a pro-inflammatory state and exacerbate disease progression in an animal model of Parkinson's disease. Central lipopolysaccharide injection in a degenerating SN exacerbated neurodegeneration, accelerated and increased motor signs and shifted microglial activation towards a pro-inflammatory phenotype with increased interleukin-1β (IL-1β) secretion. Glucocorticoid treatment and specific IL-1 inhibition reversed these effects. Importantly, chronic systemic expression of IL-1 also exacerbated neurodegeneration and microglial activation in the SN. *In vitro*, IL-1 directly exacerbated 6-OHDA-triggered dopaminergic toxicity. *In vivo*, we found that nitric oxide was a downstream molecule of IL-1 action and partially responsible for the exacerbation of neurodegeneration observed. Thus, IL-1 exerts its exacerbating effect on degenerating dopaminergic neurons by direct and indirect mechanisms. This work demonstrates an unequivocal association between IL-1 overproduction and increased disease progression, pointing to inflammation as a risk factor for Parkinson's disease and suggesting that inflammation should be efficiently handled in patients to slow disease progression.

Keywords: Parkinson's disease; inflammation; neurodegeneration; IL-1; LPS

Abbreviations: Ad = adenoviral vector; β-gal = beta-galactosidase; DXM = dexamethasone; GSA = Griffonia Simplicifolia Lectin I Isolectin B4; IL-1 = interleukin 1; IL-1ra = IL-1 receptor antagonist; rIL-1 β = rat Interleukin 1 beta; i.v. = intravenous; LPS = lipopolysaccharide; MHC = major histocompatibility complex; SMT = *S*-methylisothiourea; TH = tyrosine hydroxylase; Veh = vehicle

Received November 9, 2007. Revised April 21, 2008. Accepted May 1, 2008

Introduction

Parkinson's disease is one of the most common progressive neurodegenerative diseases, affecting over 1% of the population over the age of 60. The main hallmark of the disease is the progressive loss of dopaminergic neurons in the substantia nigra pars compacta (SN). Activated microglia are found in the SN of Parkinson's disease brains (McGeer *et al.*, 1988; Hunot *et al.*, 1999; Hirsch *et al.*, 2003; McGeer and McGeer, 2004) and in animal models (Mirza *et al.*, 2000; Vila *et al.*, 2001; Gao *et al.*, 2002; Depino *et al.*, 2003; Ferrari *et al.*, 2006); thus, inflammatory processes have also been associated with the pathogenesis of the illness. An alternative view however, is that microglia could increase neuronal survival through the release of trophic and anti-inflammatory factors (Vila *et al.*, 2001; Hald and Lotharius, 2005). Whether microglial activation protects or exacerbates

neuronal loss is presently the subject of much debate (Vila *et al.*, 2001, Wu *et al.*, 2002; Delgado and Ganea, 2003; Sanchez-Pernaute *et al.*, 2004).

Microglial activation during neurodegeneration in Parkinson's disease and prion models was not found to be accompanied by pro-inflammatory cytokine secretion (Perry *et al.*, 2002; Depino *et al.*, 2003). However, we have observed that microglial cells produced increased mRNA levels of pro-inflammatory cytokines such as interleukin-1β (IL-1β) during neurodegeneration in the SN, but that no translation of these transcripts was observed (Depino *et al.*, 2003). These and other observations prompted the hypothesis that these 'atypical' microglial cells are 'primed' cells. Hypothetically, these 'primed' microglia cells could be stimulated to adopt a potent neurotoxic pro-inflammatory phenotype by a second stimulus and exacerbate neurodegeneration (Cunningham *et al.*, 2005; McColl *et al.*, 2007). It is also well known that systemic inflammatory mediators can induce the synthesis of cytokines within the brain, suggesting that this second stimulus could have its genesis in the periphery (Besedovsky and del Rey, 1996; Pitossi *et al.*, 1997).

Here we found that a second, pro-inflammatory stimulus in the degenerating SN switches 'primed' microglia to a pro-inflammatory phenotype, which leads to increased neurodegeneration and earlier motor symptoms in a Parkinson's disease model. In addition, we have observed increased IL-1β production when lipopolysaccharide (LPS) was injected into the SN that has been previously exposed to 6-hydroxydopamine (6-OHDA). The exacerbation of the pro-inflammatory neurodegeneration and motor symptoms were all inhibited by dexamethasone (DXM) and anti-IL-1-specific treatments. Importantly, chronic, adenoviral-mediated systemic IL-1 expression was also able to exacerbate neurodegeneration in the SN, extending the relevance of the effects of inflammation on neurodegeneration to a more frequent scenario in the clinic. We also showed that IL-1 could directly exacerbate 6-OHDA toxicity to dopaminergic neurons *in vitro*. Finally, we have observed that nitric oxide was induced downstream from IL-1 production, and that its blockade partially inhibited the exacerbation on neurodegeneration observed *in vivo*. These last two results indicate that IL-1 is exerting its exacerbating effect on 6-OHDA toxicity by direct and indirect mechanisms.

Methods

Vectors

Adenoviral vectors were generated, quality controlled, and used as described previously (Kolb *et al.*, 2001; Ferrari *et al.*, 2004; Battista *et al.*, 2006). Briefly, for construction of AdIL-1, human IL-1β cDNA was cloned into a shuttle vector under the control of a human cytomegalovirus promoter and co-transfected on 293 cells with a plasmid containing E1- to E3-deleted type 5 adenoviral genome. The correct recombination was verified with restriction digestions of the purified viral DNA obtained by HIRT. Stocks were obtained from large-scale preparations in HEK293 cells by double cesium chloride gradients and were quantified by plaque assay (final titers: Ad β-gal = 5.56×10^{11} pfu/μl, Ad IL-1 = 3.85×10^{12} pfu/μl, Ad IL-1ra = 1.75×10^{12} pfu/μl). Stocks had <1 ng/ml of endotoxin, assayed with E-TOXATE® Reagents (Sigma, St Louis, Mi, USA). Viral stocks were free of autoreplicative particles as assessed by PCR and transduction of non-transcomplementary cells (HeLa, ATCC). The adenoviral vector expressing β-galactosidase (Adβ-gal) was kindly provided by Dr J. Mallet (Hospital Pitie Salpetriere, Paris).

Animals and surgical procedures

One hundred and seventy-eight adult male Wistar rats (250–300 g), were housed in groups of five animals, under controlled temperature (22 ± 2°C) and artificial light under a 12 h cycle period and with water and food *ad libitum*. All animal procedures were performed according to the rules and standards of German animal law and the regulations for the use of laboratory animals of the National Institute of Health, USA. Animal experiments were approved by the Ethical Committee of the Institute Leloir Foundation.

For stereotaxic injections, the animals were anaesthetized with ketamine chlorhydrate (80 mg/kg) and xylazine (8 mg/kg) and then injected in the left striatum with 20 ug 6-OHDA (Sigma dissolved in 4 ul saline supplemented with 0.2 mg/ml L-ascorbic acid) or vehicle only, using a 10-ul Hamilton syringe. Twelve days after they were injected, using 50 μm tipped finely drawn glass capillary containing 0.09 μg lipopolysaccharide (LPS; strain 0111:B4, Sigma–Aldrich, MA, USA diluted in 2 μl phosphate buffer (PB) or vehicle in the left substantia nigra.

The stereotaxic coordinates of the left striatum were: bregma + 1.0 mm; lateral + 3.0 mm; ventral –4.5 mm (Depino *et al.*, 2003) and the coordinates of the left SN were bregma –5.3 mm; lateral + 2mm; ventral –7.2 mm) (Paxinos and Watson, 1986). Striatal injections of 4 μl 6-OHDA or vehicle were infused over 8 min and the needle tip kept in place for additional 2 min before removal. Nigral injections of 2 μl LPS or vehicle were infused over 8 min and kept in place for additional 2 min. The animals were killed at 21 days post-6-OHDA surgery.

The adenoviral injection took place three days before 6-OHDA. The coordinates of the left MFB were: bregma –3.6 mm; lateral + 2.0 mm; ventral –8.6 mm. (Paxinos and Watson, 1986). IL-1ra-expressing and β-galactosidase-expressing adenoviral vectors were diluted in sterile 10 mM Tris–HCl, 1 mM $MgCl_2$ (pH = 7.8) and administered at a dose of 1×10^9 pfu/rat.

The Dexamethasone group received a daily intraperitoneal (i.p.) dose of Dexamethasone (1×10^{-8} M, Bruber Lab, Argentina) beginning just after LPS or vehicle injection.

In order to assess the possible contribution of iNOS, a group of animals were administered daily with 10 mg/kg i.p. of a selective and potent iNOS inhibitor *S*-methylisothiourea (SMT-Sigma, Germany) beginning 15 min before LPS or vehicle injection (Iravani *et al.*, 2002).

Systemic stimuli

Seven days after 6-OHDA was injected in the striatum, as previously described, the animals were intravenously injected with 1.36×10^9 pfu/rat of adenoviral vector producing human IL-1β or

vehicle diluted in 300 µl of sterile 10 mM Tris–HCl, 1 mM $MgCl_2$ (pH = 7.8) followed by 300 µl of saline solution. Blood samples were obtained from each group at day zero and at day twelve to ascertain total leucocyte count.

Behavioural tests

Adjusting steps test

[Animals per group: 6-OHDA/LPS (9), 6-OHDA/Veh (6), Veh/LPS (12), Veh/Veh (7), 6-OHDA/LPS + DXM (5), 6-OHDA/Veh + DXM (5), Veh/LPS + DXM (4)]. This test was performed according to Olsson *et al.* (1995) for assessment of akinaesia in the unilateral Parkinson model. Briefly, the rat was held by the experimenter with one hand fixing the hind limbs and slightly raising the hind part above the surface with one paw touching the surface. The animal was moved slowly sideways (5 s for 0.9 m), first in the forehand (right–left direction) and then in the backhand (left–right) direction for each paw. The sequence of testing was right (contralateral) paw forehand and backhand adjusting stepping, followed by left (ipsilateral) paw backhand and forehand directions. The number of the steps was counted for both paws in both directions. The experimenter handled rats at least three times before surgery to familiarize the animal with the test. In this period, animals are accustomed to the experimenter and to the testing position. The last assay before surgery was considered the pre-lesion stepping test.

Cylinder test

[Animals per group: 6-OHDA/LPS (9), 6-OHDA/Veh (8), Veh/LPS (12) and Veh/Veh (8)]. Forelimb akinaesia was assessed using the test described by Schallert *et al.* (1993). This test evaluates the use of the forelimb to support the body against the walls of a cylinder. To perform this test, the rats were put individually in an acrylic cylinder (20 cm × 30 cm). The test was performed between 16:00 and 19:00 h. The number of wall contacts performed independently with the left and the right forepaw were counted.

Histology

The animals were deeply anesthetized and transcardially perfused with heparinized saline followed by cold 4% paraformaldehyde in 0.1 M phosphate buffer (PB) (pH = 7.2). After removing the brains, they were placed in the same fixative overnight at 4°C. Then, the tissues were cryoprotected by immersion in 30% sucrose, frozen in isopentane and serially sectioned in a cryostat (40 µm) throughout the SN in the coronal plane. The 40 µm sections were used either for cresyl violet staining or for free floating immunohistochemistry.

Immunohistochemistry

Free-floating sections were incubated in blocking buffer (1% donkey serum, 0.1% Triton in 0.1 M PB) for 45 min, rinsed in 0.1% Triton in 0.1 M PB and incubated overnight with primary antibodies diluted in blocking solution. The antibodies used were: anti-Tyrosine hydroxylase (TH) for dopaminergic neurons (diluted 1 : 1000; Chemicon, Temecula, CA, USA) anti ratIL-1β (1 : 300; NIBSC, Potters Bar, UK), ED1 (1 : 200; Serotec, Raleigh, NC), MHC II (Serotec, Raleigh, NC) and the biotinylated lectin *Griffonia simplicifolia* (GSA-$1B_4$, 1 : 100; Vector Laboratories, Burlingame, CA, USA), for transforming microglial cells (Kaur and Ling, 1991), GFAP (for astrocytes 1 : 700, DAKO), anti-iNOS (1 : 100; Chemicon, UK) and anti-3-NT (1 : 100; Upstate, USA). For immunohistochemical identification of dopaminergic neurons, after three washes, the sections were incubated with donkey-anti-rabbit-biotin-conjugated antibody (Jackson, ImmunoResearch Laboratories Inc., West Grove, PA) followed by Vectastain standard ABC kit (Vector Laboratories, Burlingame, CA, USA) and developed with 3.3′ diaminobenzidine (Sigma, Saint Louis, MI, USA). Sections were mounted on DPX (Fluka, Buchs, Switzerland). For double-labeling immunohistochemistry, after three 5 min washes with 0.1 M PB, the sections were incubated with either indocarbocyanine Cy3 (Cy3)-conjugated donkey anti-mouse antibody (1 : 250; Jackson ImmunoResearch Laboratories Inc, West Grove, PA, USA), cyanine Cy2 (Cy2)-conjugated donkey anti-rabbit antibody (1 : 250; Jackson ImmunoResearch Laboratories, Inc, West Grove, PA, USA) or Cy2 conjugated streptavidin (1 : 250; Jackson ImmunoResearch Laboratories, Inc, West Grove, PA, USA) for 2 h, rinsed in 0.1 M PB and mounted in Mowiol (Calbiochem, San Diego, CA, USA). Digital images were collected in a Zeiss LSM 510 laser scanning confocal microscope equipped with a krypton-argon laser.

Quantitation

Quantitation of dopaminergic neurons, TH- positive cells were counted through the whole SN pars compacta at 20 × magnification. Every sixth 40-µm-thick section of each SN of every rat was counted (from 8 to 10 sections per animal, usually nine sections per rat). Sections were counted twice using double-blind procedure. Graphs show the ratio between the ipsilateral hemisphere versus the contralateral one [Animals per group for central stimulus: 6-OHDA/LPS (7), 6-OHDA/Veh (9), Veh/LPS (5) and Veh/Veh (4); central stimulus with DXM treatment 6-OHDA/LPS + DXM (5), 6-OHDA/Veh + DXM (4), Veh/LPS + DXM (4) and Veh/Veh + DXM (4); central stimulus with adenoviral inhibition of IL-1 Ad IL-1ra/6-OHDA/LPS (6), Ad β-gal/6-OHDA/LPS (5), Ad IL-1ra/6-OHDA/Veh (4), Ad β-gal/6-OHDA/Veh (4), Ad IL-1ra/Veh/LPS (4), Ad β-gal/Veh/LPS (4); systemic stimulus 6-OHDA/Ad IL-1βiv(7), 6-OHDA/Ad β-gal iv (6), Veh/Ad IL-1βiv (9) and Veh/Ad β-gal iv (8)].

For the quantitation of MHCII positive cells, cells stage 4 were identified by their morphology on MHCII staining under 40 × magnification and counted in every sixth 40-µm-thick serial section of the SN of each rat using a double-blind procedure. Graphs show the number of MHCII positive cells in the SN.

[Animals per group for central stimulus: 6-OHDA/LPS (4), Veh/LPS (4); central stimulus with DXM treatment 6-OHDA/LPS + DXM (3), Veh/LPS + DXM (3); central stimulus with adenoviral inhibition of IL-1 Ad IL-1ra/6-OHDA/LPS (3), Ad β-gal/6-OHDA/LPS (3), Ad IL-1ra/Veh/LPS (3), Ad β-gal/Veh/LPS (3); systemic stimulus 6-OHDA/Ad IL-1βiv(5), 6-OHDA/Ad β-gal iv (4), Veh/Ad IL-1βiv (5) and Veh/Ad β-gal iv (5)].

Classification of microglial activation

We adopted the classification of microglial activation according to Kreutzberg (1996) Stages of microglia activation were confirmed by observation by at least two different observers.

See yellow circles in Fig. 3 (A′, A″, A‴) for examples of different stages of microglial activation.

Stage 1: Resting microglia. Rod shaped soma with fine and ramified processes.
Stage 2: Activated ramified microglia. Elongated shaped cell body with long and thicker processes.
Stage 3: Amoeboid microglia. Round shaped body with short, thick and stout processes.
Stage 4: Phagocytic cells. Round shaped cells with vacuolated cytoplasm, no processes can be observed at light microscopy level.

All these cellular types are GSA positive (GSA +). ED1 and MHC-II are capable of staining activated but not resting microglia.

ELISA for IL-1β, TNF and IL-6

Animals were decapitated and their brains were quickly removed and both the injected and non-injected SN were dissected, snap-frozen in liquid nitrogen and stored at –80°C. Tissue was homogenized on ice in 400 µl of Tris–HCl buffer (pH = 7.3) containing protease inhibitors (10 µg/ml aproteinin, 5 µg/ml peptastin, 5 µg/ml leupeptin, 1 mM PMSF). Homogenates were centrifuged at 10 000*g* at 4°C for 10 min and then ultracentrifuged at 40 000 r.p.m. for 2 h. Samples were aliquoted and stored at –80°C until use. Bradford protein assays were performed to determine total protein concentration in each sample. Commercially available rat IL-1β, rat TNF-α and rat IL-6 kits (R&D, Minneapolis, MN, USA) with high sensitivity were used to quantify these cytokines according to the manufacturers' instructions (15 pg/ml for rIL-1β and 7.8 pg/ml for rTNF-α and rIL-6). Five to ten animals per group were analyzed and each sample was in duplicate. To estimate protein recovery, rIL-1β standard was added exogenously to brain homogenates and the ELISA was performed as described before. A recovery of 85–90% of the added rIL-1β standard was found. Animals per group: central stimulus 6-OHDA/LPS (10), 6-OHDA/Veh (10), Veh/LPS (9) and Veh/Veh (7); central stimulus with DXM treatment 6-OHDA/LPS + DXM (5) and Veh/LPS + DXM (5); central stimulus with SMT treatment 6-OHDA/LPS + SMT (6), 6-OHDA/Veh + SMT (6), Veh/LPS + SMT (6).

Neuronal cell cultures and cell viability assay (MTT)

SK-N-SH (HTB-11, human brain neuroblastoma) cells were cultured in RPMI 1640 (Gibco, Scotland, UK) supplemented with 10% fetal bovine serum (Natocor). Cells were grown to confluence at 37°C in 5% CO_2.

For mitochondrial tetrazolium assay (MTT) procedure, cells were seeded 1×10^4 cells/well in 96-well tissue culture plates. Twenty-four hours later, cells were exposed to 6-OHDA solution (3.125 µM) diluted in culture medium. After 24 h of incubation, the medium was aspirated to be replaced by 100 µl/well of different concentrations of IL-1 (0.125, 0.0625, 0.05 and 0.03 pg/µl) and incubated for another 24 h. Then, 10 µl/well of MTT solution (5 mg/ml PBS) was added and incubated at 37°C for 4 h. Finally, 100 µl of isopropanol/0.04N HCl was added to each well. After mixing thoroughly by repeated pipetting with a multichannel pipettor, the plate was measured at 570 nm using an ELISA plate reader (BIO-RAD Model 550, microplate reader). The test was carried out in two independent experiments, each tested in triplicate.

RNA isolation, reverse transcription and real-time PCR (RT-PCR)

Animals were decapitated and their brains were quickly removed and both SN were dissected, snap-frozen in liquid nitrogen and stored at –80°C. Total RNA was prepared by homogenizing nigral tissue in 700 µl of TRI Reagent (Sigma, USA). One microlitre of Linear Acrylamide (5 mg/ml) (Ambion) was added as a carrier and the mixture was extracted with 140 µl of chloroform. The aqueous phase was precipitated with 400 µl isopropanol and resuspended in 20 µl of RNAse-free milliQ water. Reverse transcription was performed by incubating 10 µg of the RNA with 1 µl oligo-dT (Invitrogen) and 1 µl of SuperScript First-strand Synthesis System for RT-PCR (Invitrogen), according to manufacturer's protocol.

For quantitative RT-PCR reaction, 23 µl of SYBR Green Master Mix was added to 2 µl of cDNA. The SYBR Green Master Mix consisted of: 3 mM MgCl2, 2.5 µl of 10 × PCR buffer, 0.3 mM dNTPs, 0.01 mM Rox Dye, 0.1 mg/ml BSA, 0.75 µl of 10 × SYBR Green (Molecular Probes), 0.25 µl Platinum *Taq* Polymerase (Invitrogen, Life Technologies) and of either β2-microglobulin or COX2, forward and reverse primers (0.2 mM). Quantitative RT-PCR was performed on an iCycler IQTM Real Time PCR Detection System, (Bio-Rad). Reaction conditions were as follows: 2.5 min at 94°C, 42 cycles of 45 s at 94°C, 1 min at 54°C, 1 min at 72°C and 3 min at 72°C. The specificity of PCR primers was tested, and a single DNA band of the expected molecular size was observed in a 1.5% agarose gel electrophoresis stained with ethidium bromide. In addition, a single peak in the iCycler plot was observed after a melting curve was performed. Primers for β2-microglobulin were as follows forward, TCTTTCTGGTGCTTG TCTC and reverse, AGTGTGAGCCAGGATGTAG and COX2 forward, TACCCGGACTGGATTCTACG and reverse, AAGTTGG TGGGCTGTCAATC. Each sample was tested in triplicate. To compare mRNA expression between treatments, the amount of mRNA was expressed as the ratio of COX2/β2-microglobulin levels.

Statistical analysis

Results are expressed as mean ± SEM in the different treatment groups.

All experiments were analyzed by analysis of variance (ANOVA) followed by Fisher's protected least significant difference (LSD) as *post hoc* test. To make sure parametric statistical analysis could be carried out, all variables were tested for normality and variance homogeneity with Kolmogorov–Smirnov and Levene test, respectively. In two cases, data had to be transformed to conform to these statistical requirements (Figs 4 and 6D).

The criteria used for the choice of statistical test to analyze the data were determined by the number of factors present in the experiment (Two or three-way ANOVA). When one of the levels of any factor was missing, one-way ANOVA was performed considering each experimental group as a different treatment. Three-way ANOVA and repeated measures (day) was used when multiple measurements were performed on the same animal, as in the case of the behavioural tests.

All *post hoc* test were carried out with Fisher's protected LSD test (least significant difference) and the level of statistical significance was set at $P < 0.05$. For clarity, statistical analyses of each test are addressed in each figure. All statistical tests were performed using SPSS 11.0 for Windows (SPSS, Inc., Chicago, Il, USA).

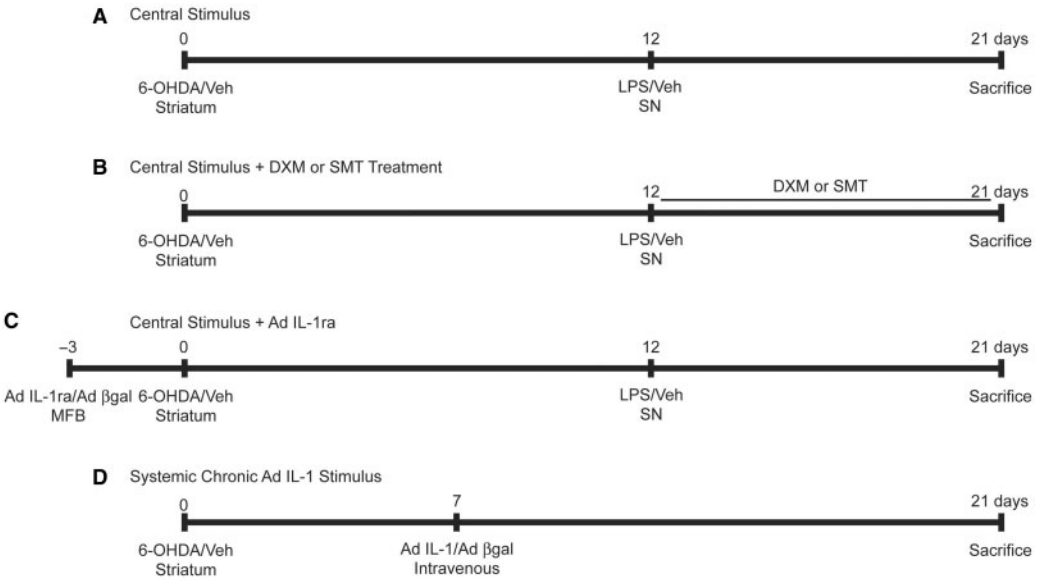

Fig. 1 Timeline for central or systemic stimulus. Experimental groups were divided into: (**A**–**C**) 'Central stimulus' with rats intrastriatally injected with 6-OHDA and LPS (6-OHDA/LPS) or vehicle (6-OHDA/Veh) at Day 12 into the SN. Rats intrastriatally injected with Vehicle and LPS (Veh/LPS) or vehicle (Veh/Veh) at day 12 into the SN (**A**). (**B**) The dexamethasone (DXM) group received a daily intraperitoneal dose of 10^{-8} M of DXM starting just after the LPS or vehicle stereotaxical injection or 10 mg/kg of *S*-methylisothiourea SMT 15 min prior to LPS or vehicle injection and daily after that. (**C**) In the IL1 activity blockade experiments, animals were injected with Ad IL-1ra or Ad β-gal in the MFB three days prior to 6-OHDA intrastriatal injection. (**D**) 'Systemic stimulus' with rats intrastriatally injected with 6-OHDA and intravenously with Ad IL1β (6-OHDA/Ad IL1β iv) or vehicle (6-OHDA/Ad β-gal iv) at Day 7 in the tail vein. Rats intrastriatally injected with Vehicle and intravenously with Ad IL1β (Veh/Ad IL1βiv) or Ad β-gal (Veh/Ad β-gal iv) in the tail vein.

Results

Central LPS administration exacerbates ongoing 6-OHDA-mediated neurodegeneration in the SN

To test whether inflammation can exacerbate ongoing neurodegeneration in the SN, we first injected different doses (range 0.06–2 μg) of lipopolysaccharide (LPS) into the SN and observed that 0.09 μg of LPS was able to produce microglial activation without overt neurodegeneration in that area (data not shown). Then, 12 days after injecting animals with 6-OHDA or vehicle in the striatum (Sauer and Oertel, 1994), we administered LPS or vehicle in the SN as shown in Fig. 1A. This time point was chosen because neurodegeneration has begun in the SN at 12 days and we have previously found that microglial cells are 'primed' at this point with increased pro-inflammatory cytokine transcription, but without translation (Depino *et al.*, 2003).

We quantified the surviving dopaminergic cells in the SN in each experimental group 21 days after the 6-OHDA or after vehicle injections (Fig. 2A) and found a statistically significant decrease in the number of tyrosine hydroxylase (TH) positive cells in the whole SN in animals treated with 6-OHDA/LPS in comparison with the other groups (6-OHDA/Veh, Veh/LPS, Veh/Veh) (Fig. 2A, $P<0.001$). There was no significant decrease in TH-positive cells when comparing animals injected with LPS in an intact SN (Veh/LPS) with the LPS control group (Veh/Veh) (Fig. 2A). In particular, the combined treatment (neurodegenerative and inflammatory) in the 6-OHDA/LPS group produced more neurodegeneration (54.43%) than the effects of the neurodegenerative treatment (6-OHDA/Veh) (31.67%) and the inflammatory treatments separately (Veh/LPS) (13.75%), indicating an exacerbating effect of the LPS on the degenerating SN.

As a functional control of the exacerbating effect of LPS on the ongoing neurodegeneration, we administered dexamethasone (DXM), a well-known anti-inflammatory steroid, from days 12 to 20 to experimental groups described (Fig. 1B). DXM treatment suppressed the reduction in TH-positive cells in the SN in the 6-OHDA/LPS group up to levels obtained in the 6-OHDA/Veh group (Fig. 2A, $P<0.001$ 6-OHDA/LPS+DXM versus 6-OHDA/LPS-DXM). There were no effects of DXM observed in the 6-OHDA/Veh group suggesting that DXM had no effect on 6-OHDA neurodegeneration *per se*. A marginal effect of DXM was observed in the Veh/LPS group, attributable to a DXM-mediated reduction of a minor local effect of LPS, the Vehicle injection or both. This result suggests that DXM treatment prevents the loss of TH-positive cells by blocking the inflammation produced by LPS.

Central LPS administration exacerbates and accelerates detectable 6-OHDA-mediated motor deficits

In order to test whether the LPS-elicited inflammatory reaction in the SN could exacerbate motor symptoms

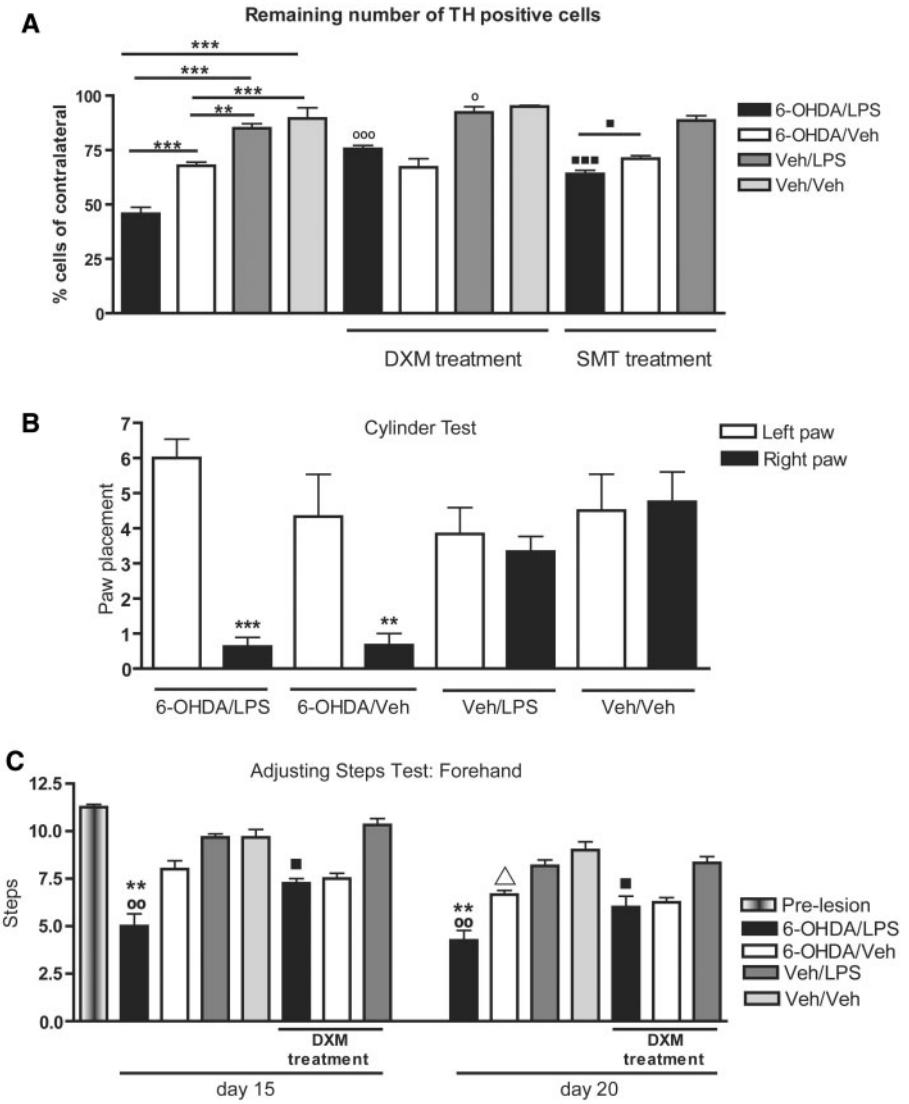

Fig. 2 (**A**) Remaining number of TH positive cells in the SN 21 days after different central treatments. Quantitation of TH positive cells as a percentage of cells in the ipsilateral hemisphere versus the contralateral one. Two-way ANOVA (significant double interaction $P<0.05$) was followed by Fisher's LSD *post hoc* test. $^{***}P<0.001$ 6-OHDA/LPS compared to 6-OHDA/Veh, Veh/LPS and Veh/Veh group. $^{**}P<0.01$ 6-OHDA/Veh compared to Veh/LPS. $^{***}P<0.001$ 6-OHDA/Veh compared to Veh/Veh. Error bars represent SEM. ($N=7$, 9, 5 and 4 for 6-OHDA/LPS, 6-OHDA/Veh, Veh/LPS and Veh/Veh groups, respectively). DXM group: Three-way ANOVA (significant triple interaction $P<0.01$) was followed by Fisher's LSD *post –hoc* test. $^{\circ\circ\circ}P<0.001$ significant difference between 6-OHDA/LPS+DXM and 6-OHDA/LPS-DXM. $^{\circ}P<0.05$ significant difference between Veh/LPS+DXM and Veh/LPS-DXM. Error bars represent SEM. ($N=5$, 4, 4 and 4 for 6-OHDA/LPS+DXM, 6-OHDA/Veh+DXM, Veh/LPS+DXM and Veh/Veh+DXM groups, respectively). SMT group: One-way ANOVA was followed by Fisher's LSD *post hoc* test. $^{\blacksquare\blacksquare\blacksquare}P<0.001$ significant difference between 6-OHDA/LPS+SMT and 6-OHDA/LPS-SMT. $^{\blacksquare}P<0.05$ significant difference between 6-OHDA/LPS+SMT and 6-OHDA/Veh+SMT. Error bars represent SEM. ($N=6$, 4 and 5 for 6-OHDA/LPS+SMT, 6-OHDA/Veh+SMT and Veh/LPS+SMT groups, respectively). (**B** and **C**) Motor behavioural deficits after central treatments and the effects of anti-inflammatory agent on behavioural tests. (**B**) Cylinder test. The number of first paw placement on the surface of a cylinder was counted for each experimental group. Three-way ANOVA (significant striatum—paw double interaction $P<0.001$) was followed by Fisher's LSD *post hoc* test. $^{***}P<0.001$ when comparing 6-OHDA/LPS between left and right paws. $^{**}P<0.01$ when comparing 6-OHDA/Veh between left and right paws. Error bars represent SEM. ($N=9$, 8, 12 and 8 for 6-OHDA/LPS, 6-OHDA/Veh, Veh/LPS and Veh/Veh groups, respectively). (**C**) Adjusting steps test at 15 and 20 days after 6-OHDA or Vehicle injection (pre-lesion measurements were carried out for every animal). Performance with the left paw (ipsilateral to the lesion) presented no difference in both directions (data not shown). Only performance with the right paw was impaired in both directions (backhand direction not shown). Three-way ANOVA (Striatum, SN and day with repeated measures for the last factor) was followed by Fisher's LSD *post hoc* test. $^{\circ\circ}P<0.01$, significant difference between 6-OHDA/LPS group and the pre-lesion measurement. $^{**}P<0.01$ significant difference among 6-OHDA/LPS group and other groups (6-OHDA/Veh, Veh/LPS and Veh/Veh) within the same time point. $^{\triangle}P<0.05$ difference among 6-OHDA/Veh group and other control groups (Veh/LPS and Veh/Veh) for Day 20. $^{\blacksquare}P<0.05$ significant difference between 6-OHDA/LPS group with or without DXM treatment at each time point (Day 15 and Day 20). Error bars represent SEM. ($N=9$, 6, 12, 7, 5, 5 and 4 for 6-OHDA/LPS, 6-OHDA/Veh, Veh/LPS, Veh/Veh, 6-OHDA/LPS+DXM, 6-OHDA/Veh+DXM, Veh/LPS+DXM groups, respectively).

in the 6-OHDA-treated animals, two behavioural tests were performed during the period of ongoing neurodegeneration.

Cylinder test

The treatment with 6-OHDA produced a marked and statistically significant difference in the placement of the contralateral paw on the cylinder's surface that was independent of other treatments (Fig. 2B, 6-OHDA/LPS and 6-OHDA/Vehicle versus the other two groups, $P<0.001$ when comparing 6-OHDA/LPS between left and right paws, $P<0.01$ when comparing 6-OHDA/Veh between left and right paws). The total number of first paw placements was not altered between groups (Fig. 2B). Thus, this test was very sensitive to the 6-OHDA effect independently of any subsequent treatment.

Adjusting steps test

At 15 days, the 6-OHDA/LPS group, but not any of the other groups, showed a significant decrease in the number of adjusting steps with the right paw (contralateral to the lesion) in both directions (Fig. 2C, $^{\circ\circ}P<0.01$ when compared 6-OHDA/LPS to pre-lesion measurement, $^{**}P<0.01$ when compared 6-OHDA/LPS to other groups, backhand direction not shown). Thus, the effect of the administration of LPS in the SN on the 6-OHDA-injected animals elicited motor disabilities sooner than in the other groups. In addition, at 20 days post 6-OHDA inoculation, the 6-OHDA/LPS animals showed increased motor disabilities when compared to the 6-OHDA/Veh group (Fig. 2C, $^{**}P<0.01$). This result suggests that LPS elicited motor disabilities earlier in the pathogenesis and also increased motor symptoms, in agreement with the increased neurodegeneration observed previously in this group. The Veh/LPS and Veh/Veh groups showed no motor impairments (Fig. 2C), as expected from the number of TH-positive cells in the SN remaining in each animal at that time point. Thus this test demonstrated the exacerbation of motor symptoms in the 6-OHDA/LPS treated group.

In order to address the question as to whether the attenuation of inflammation could prevent the exacerbation of motor symptoms, we performed the same behavioural test with the same DXM treatment as described previously. Dyskinaesia associated with LPS-triggered exacerbation was reversed in animals treated with DXM (Fig. 2C, $^{\blacksquare}P<0.05$ 6-OHDA/LPS+DXM versus 6-OHDA/LPS-DXM). The number of adjustment steps in the 6-OHDA/LPS group increased with respect to the same group without DXM up to the level of 6-OHDA/Veh group. This result was again in agreement with the number of TH-positive cells remaining. As expected, there were no differences in the control groups after DXM treatment (6-OHDA/Veh, Veh/LPS-Fig. 2C). These results provide functional evidence that the LPS-triggered inflammation resulted in exacerbation of motor disabilities in the 6-OHDA-treated animals.

Primed microglial cells are markedly shifted to a pro-inflammatory stage in the 6-OHDA/LPS animals only

Microglial cells are the main modulators of inflammation in the brain. In the 6-OHDA model, activated microglial cells exhibit morphological changes defined as stage 3, but not stage 4 (Depino *et al.*, 2003). We studied the morphological changes associated with microglial activation by staining with the microglia marker Griffonia Simplicifolia Lectin I Isolectin B4 (GSA) and by the detection of specific markers such as ED-1 and MHC class II expression. In animals treated with 6-OHDA/LPS, mainly stage 4, ED-1-positive microglia was visualized by GSA-staining in the whole SN. (Fig. 3A and D, see yellow circles for a higher magnification and detailed description of microglial activation (Fig. 3A′, A″ and A‴). MHC class II-positive cells showed similar morphological stages of activation to GSA labelling, but the distribution of the label was more restricted to the lesion (Fig. 3G). In contrast, only stages 2–3 of microglial phenotype with sparse ED-1 and MHC II-reactivity along the injection tract were observed in the SN of 6OHDA/Veh group (Fig. 3B, E and H and data not shown). In the animals injected with LPS only in the SN (Veh/LPS), the vast majority of microglia presented morphology consistent with stage 2 or 3 while stage 4, ED-1 and MHCII-positive cells were rare and only observed at the injection site (Fig. 3C, F and I). Thus, this dose of LPS could only marginally drive microglia phenotype to stage 4 at the injection site (<240 μm rostrocaudally within the SN), but the same LPS dose injected into rats previously treated with 6-OHDA led to a massive change of microglial morphology (mainly stage 4 at least 1920 μm across the SN). Rats treated with Veh/Veh, showed minor microglial phenotype changes (stages 1–2) at the capillary tract. Thus, these data suggest that only LPS administration in the neurodegenerating SN shifted the microglial phenotype to stage 4, ED-1, MHCII-positive cells.

We also studied the potential involvement of astrocytes by performing immunohistochemistry against GFAP in the SN of 6-OHDA/LPS, 6-OHDA/Veh, Veh/LPS animals. We found no induced expression of GFAP in the SN pars compacta of any experimental group, suggesting a minor participation of astrocytes in the exacerbating effect of LPS and highlighting the relevance of microglial activation in this model (data not shown).

It is known that DXM treatment downregulates microglial activation and, in particular, MHC class II expression in microglial cells *in vitro* and *in vivo* (Kiefer and Kreutzberg, 1991). DXM treatment reduced MHC class II expression in animals treated with 6OHDA/LPS or Veh/LPS (Fig. 3, compare G and I with N and O, respectively). The number of stage 4, MHC class II-positive cells was reduced by >50% after DXM treatment (Fig. 3P, $^{**}P<0.01$ 6-OHDA/LPS+DXM versus 6-OHDA/LPS-DXM). By contrast, GSA and ED-1 staining seemed to be not altered with

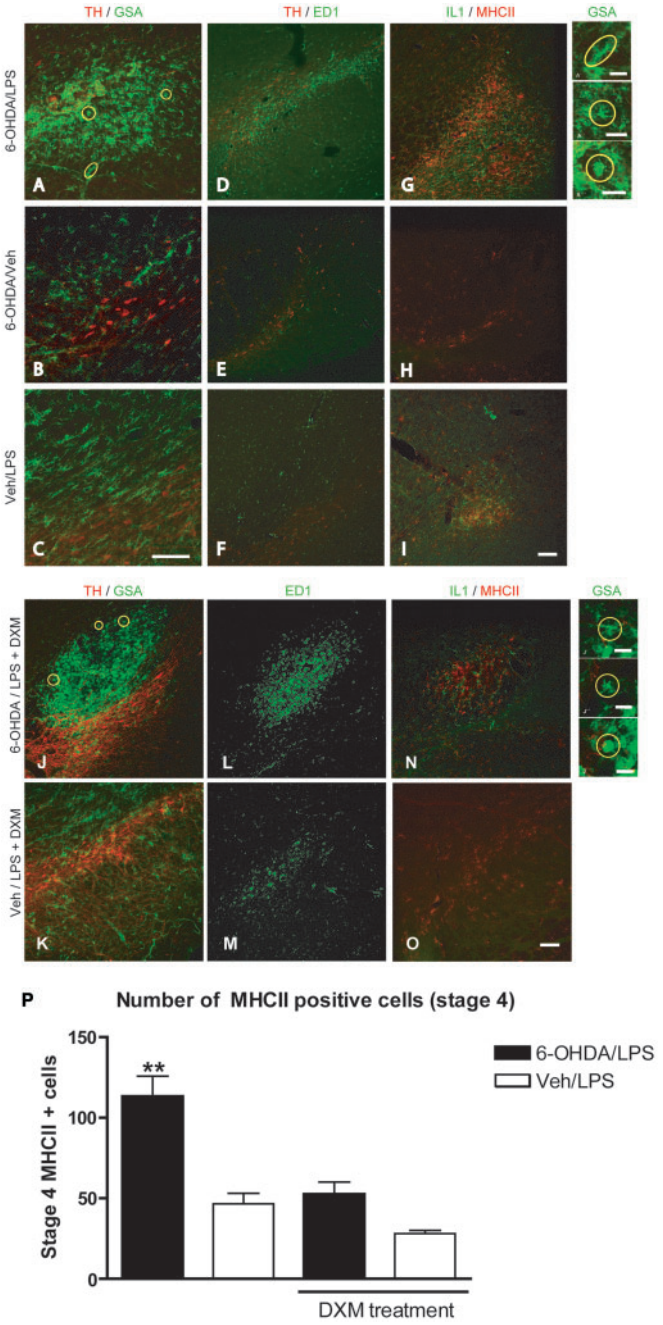

Fig. 3 Activation of microglial cells in the SN after different central treatments **(A–I)** DXM-treated groups are also shown **(J–P)**. **(A–C)**. Activation of microglial cells as demonstrated by GSA (green)/TH (red). **(A)**. Animals injected with 6-OHDA/LPS mostly exhibited GSA + cells at stage 4. In addition stages 2–3 microglial cells can be observed surrounding the SNpc. The animals injected with 6-OHDA/Veh (**B**) and Veh/LPS (**C**) have GSA + cells at stages 2 and 3 in the SN. A′–A‴: Examples of different stages of microglial activation magnified from A (yellow circles): A′, Stage 2 characteristic rod-shaped cell. Ramified processes can be visualized; A″, Stage 3 amoeboid microglia with thick and stout processes; A‴ Stage 4 Phagocytic cell, round-shaped body. (**D–F**). Activated microglia with macrophage characteristics confirmed by EDI (green), in the SN labelled with TH (red) immunofluorescence. (**D**). EDI + cells at stage 2, 3 and 4 are observed within the SN in the 6-OHDA/LPS group. However, control groups (6-OHDA/Veh and Veh/LPS) exhibited scarce EDI labelling (**E** and **F**, respectively). **(G–I)**. Expression of the class two major histocompatibility complex (MHC-II) (red) and rat IL-1β (rIL-1β–green) in the different treatments. (**G**). Stage 4 MHC-II + cells are observed within the SN but ramified MHC-II + cells are located surrounding the lesion in 6-OHDA/LPS group. Ramified rIL-1β + cells are also observed within the lesion in this group (**G**). (**H**) Animals treated with 6-OHDA/Veh showed MHC-II + cells at stage 2. No IL-1β label was observed in this group. (**I**) Some MHC-II + cells at stage 4 can be observed at the injection site in Veh/LPS group. Stages 2 and 3 cells were also observed surrounding the injection site. Ramified rIL-1β + cells can also be seen in the same region. **(J–P)** Microglial activation after Dexamethasone treatment. (**J** and **K**) Activation of microglial cells demonstrated by GSA (green)/in the SN labeled with TH (red) staining. (**J**) The animals injected with 6-OHDA/LPS and treated with DXM showed mostly stage 4 GSA + cells in the whole SN. However, the Veh/LPS DXM treated group exhibited stage 2–3 microglial cells in the SN (**K**). J′–J‴: Examples of different stages of microglial activation magnified from J (yellow circles): J′, Stage 2 characteristic rod-shaped cell. Ramified processes can be visualized; J″, Stage 3 amoeboid microglia with thick and stout processes; J‴ Stage 4 Phagocytic cell, round-shaped body. Scale bar A′, A″, A‴ and J′, J″, J‴: 20 μm. (**L** and **M**) Activated microglia with macrophage characteristics confirmed by EDI (green) immunofluorescence. (**L**) 6-OHDA/LPS DXM treated group showed ED-1 + cells at stage 4 within the lesion site, but also exhibited microglial cells at stage 2 and 3 surrounding the SN. The control group, Veh/LPS treated with DXM mainly had ED-1 + cells at stages 2–3, but scarce cells at stage 4 can also be observed (**M**). (**N–P**). Expression of the major histocompatibility complex class two (MHC-II) (red) and rIL-1β (rat IL-1β–green) in DXM treatment. (**N**) The animals injected with 6-OHDA/LPS and DXM exhibited less MHC-II label than those observed in non-DXM-treated animals (**G**). Some cells reached stage 4, but most of them were at stages 2–3 (**N**). Ramified IL-1β + cells can also be observed within the lesion (**N**). (**O**) Stages 2 and 3 MHC-II + cells were observed in the SN of animals injected with Veh/LPS and DXM. No IL-1β label was observed in this group. Scale bar: 100 μm. (**P**) Number of MHC-II + cells at stage 4 in the SN of animals injected with 6-OHDA/LPS ($N = 4$), Veh/LPS ($N = 4$), 6-OHDA/LPS +DXM ($N = 3$) and Veh/LPS+DXM ($N = 3$). Two-way ANOVA (significant double interaction $P < 0.05$) followed by Fisher's LSD *post hoc* test. $^{**}P < 0.01$ 6-OHDA/LPS+DXM compared to 6-OHDA/LPS-DXM. Error bars represent SEM.

the DXM treatment (Fig. 3 compare A versus J and C versus K for GSA profile and D versus L and F versus M for ED-1 profile). These results identify a distinct population of activated microglial cells (MHCII-positive), that correlate with the levels of neurodegeneration and motor symptoms in the 6-OHDA/LPS group before and after DXM treatment.

The pro-inflammatory stage of microglial activation is best defined by the molecules secreted, such as the pro-inflammatory cytokines. We investigated the expression profile of three key pro-inflammatory cytokines; IL-1β, TNFα and IL-6 in the SN of rats from each experimental group at 21 days post-6-OHDA, the same time point when neurodegeneration, motor symptoms and microglial activation were examined. Interestingly, we found, using ELISA, a significant increase in the induction of IL-1β expression in rats treated with 6-OHDA/LPS in comparison with the

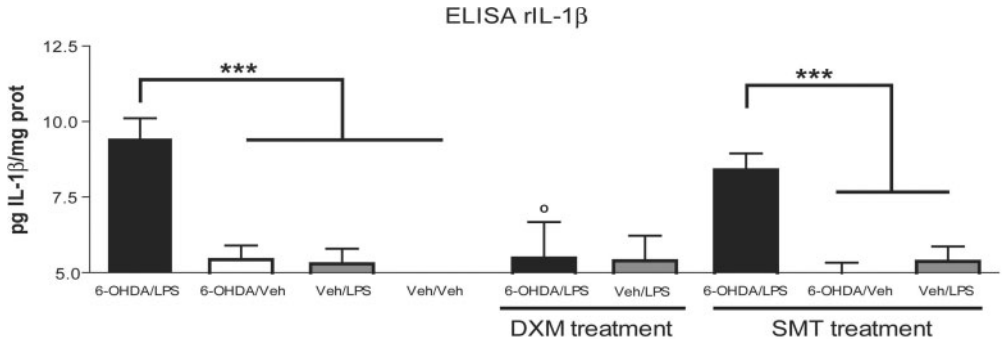

Fig. 4 IL-1β expression measured by ELISA in the SN after different treatments. Two-way ANOVA (Striatum and SN) with significant double interaction $P < 0.05$ was followed by Fisher's LSD *post hoc* test. ***$P < 0.001$ 6-OHDA/LPS ($N = 10$) compared to 6-OHDA/Veh ($N = 10$), Veh/LPS ($N = 9$) and Veh/Veh ($N = 7$). DXM group: IL-1 content in the SN by ELISA was also measured for Dexamethasone-treated animals (6-OHDA/LPS+DXM $N = 5$ and Veh/LPS+DXM $N = 5$). Two-way ANOVA (Striatum and DXM) with significant double interaction $P < 0.05$ was followed by Fisher's LSD *post hoc* test. $P < 0.05$ significant difference between 6-OHDA/LPS group with or without DXM treatment. Error bars represent SEM. SMT group: ELISA was also used to measure IL-1 in the SN of SMT-treated animals. (6-OHDA/LPS, 6-OHDA/Veh, Veh/LPS $N = 6$ for each group). After a one-way ANOVA no statistical difference was found between groups with or without SMT treatment. ***$P < 0.001$ 6-OHDA/LPS+SMT compared to 6-OHDA/Veh+SMT and Veh/LPS +SMT. The minimal amount of IL-1 depicted in the graph represents the detection threshold of the assay.

other treatments (6-OHDA/Veh, Veh/LPS and Veh/Veh) (Fig. 4, $P < 0.001$). No differences were found between the 6-OHDA/Veh, Veh/LPS and Veh/Veh groups. Immunohistochemical analysis confirmed the presence of ramified rat IL1β (rIL-1β) positive cells in the whole SN of 6-OHDA/LPS injected animals (Fig. 3G). On the contrary, rIL1β positive cells were scarce and found only at the injection site or along the capillary tract in the Veh/LPS and 6-OHDA/Veh groups respectively (Fig. 3I and H).

There were no differences in the levels of TNFα or IL 6 protein in the SN of any group (data not shown). Thus, neither of these cytokines appears to be involved in the exacerbating effects observed in the 6-OHDA/LPS animals.

IL-1β expression was markedly diminished in the 6-OHDA/LPS group with DXM treatment compared with the same group without DXM administration (Fig. 4), with levels comparable to all other experimental control groups (Fig. 4). Thus, DXM was able to inhibit the exacerbation on IL-1β synthesis by LPS on 6-OHDA-affected SN.

Inhibition of IL-1 activity in the SN leads to decreased neurodegeneration but not downregulation of microglial activation in that region

To confirm IL-1β participation in the exacerbation of the ongoing neurodegeneration by LPS, we decided to block IL1β biological activity by injecting an adenovirus expressing the natural endogenous inhibitor of IL-1, IL-1ra in the SN (Fig. 1C). We chose to inject the viral vector in the medial forebrain bundle (MFB) in order to induce IL-1ra in the SN without injecting this area twice. We know from previous results that the efficiency of transduction with control adenoviral vectors using this route of injection amounted to 30–35% of TH+ cells in the SN, leaving the SN undisturbed (data not shown). In addition, under our experimental conditions, no adenoviral vector mediated inflammation is observed in the brain 7 days after vector inoculation (Ferrari *et al.*, 2006) and this vector can efficiently inhibit IL-1 activity (Depino *et al.*, 2004).

The injection of 1×10^9 pfu of adenovirus expressing IL-1ra in the MFB of 6-OHDA/LPS animals lead to an increase in TH-positive cells in the SN when compared with similar animals injected with 1×10^9 pfu of an adenovector expressing β-galactosidase (Fig. 5A, $P < 0.001$). This rise in the number of TH-positive cells was comparable to the number of TH-positive cells left after the 6-OHDA treatment alone. No changes were seen in the 6-OHDA/Veh group as expected because of the lack of induction of IL-1β in this group (Fig. 5A). As expected, the AdIL-1ra treatment had no effect on the number of dopaminergic neurons in the SN of Veh/LPS animals (Fig. 5A), since this dose of LPS was not neurodegenerative *per se* (Fig. 2A). These results point to IL-1 as a key mediator of LPS-mediated exacerbation of neuronal loss in the degenerating SN.

IL-1-induced functional blockade did not show any effects on the stages of microglial activation in the 6-OHDA/LPS group as seen by morphological changes detected by GSA staining (Fig. 5B), ED1 immunolabelling (Fig. 5D) or MHC class II expression (Fig. 5F and H) in the SN. No effects were observed in the Veh/LPS group (Fig. 5C, E, G and H). These results suggest that IL-1β expression is a downstream event from microglial activation.

Systemic, chronic IL-1 expression exacerbated 6-OHDA-mediated neurodegeneration and drove microglia to end-stage activation in the SN

We generated an animal model of chronic systemic inflammation by injecting an adenoviral vector expressing IL1β (or β-galactosidase as control) in the tail vein of 6-OHDA

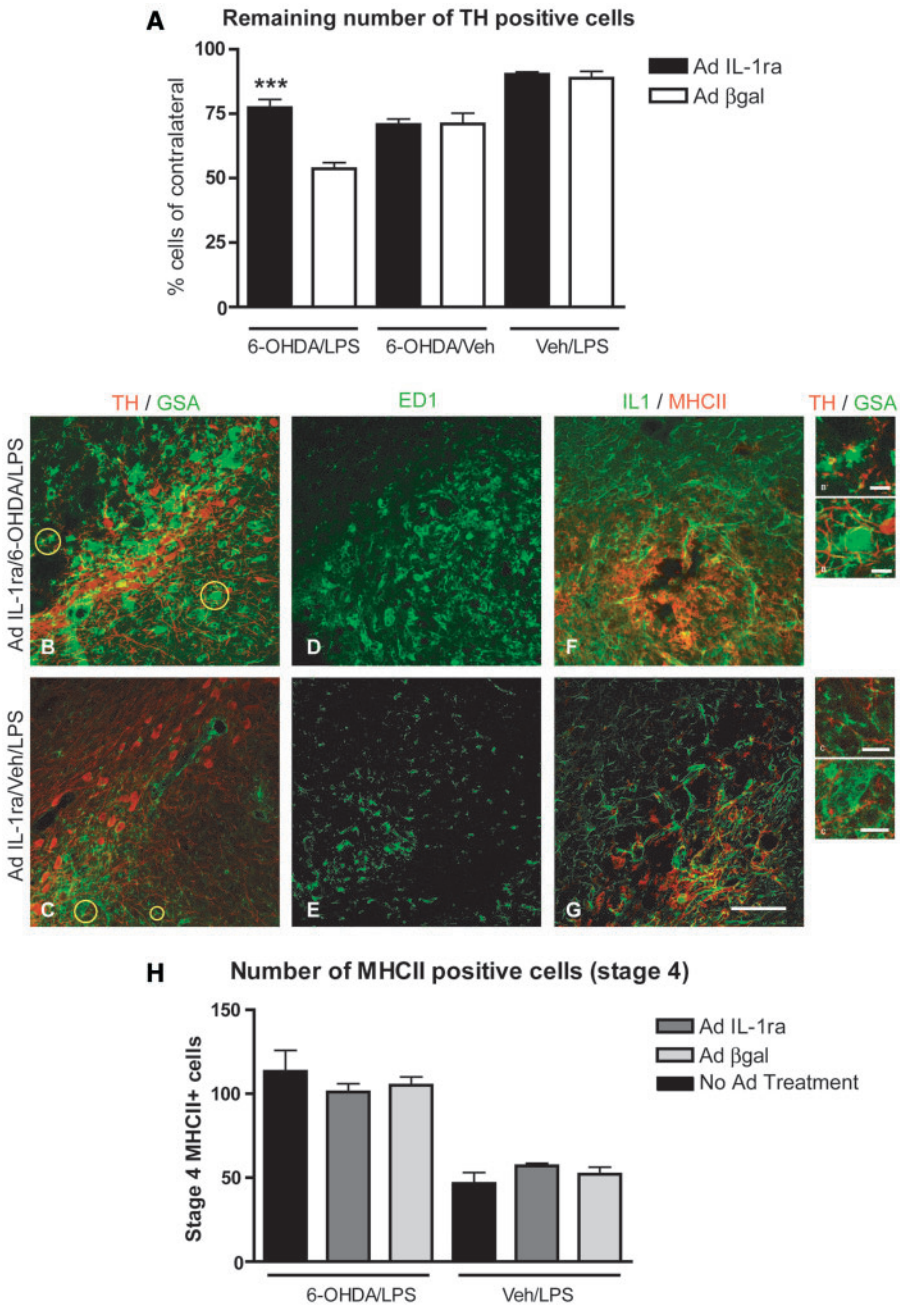

Fig. 5 Inhibition of IL-1β activity. (**A**) Quantitation of remaining TH-positive cells as a percentage of cells in the ipsilateral hemisphere versus the contralateral one. Ad IL-1ra-treated rats: filled bars, Adβ-gal-treated rats: empty bars. Significant differences were analyzed with one-way ANOVA. $^{***}P < 0.001$ significant difference between 6OHDA/LPS group treated with Ad IL-1ra or with control adenovirus (Ad β-gal). (Ad IL-1ra/6-OHDA/LPS $N = 6$, Ad β-gal/6-OHDA/LPS $N = 5$, all other groups $N = 4$). Error bars represent SEM. (**B**–**G**) Microglial activation after AdIL-1ra treatment. (**B** and **C**) Microglial activation evidenced with GSA (green) in the SN labeled with TH (red). (**B**) Morphological activation at Stage 4 was observed in the SN of animals injected with 6-OHDA/LPS and treated with AdIL-1ra. Some stage 3 cells can be observed surrounding the SNpc. (**C**) Control animals injected with Veh/LPS and AdIL-1ra exhibited few GSA+ cells only at stages 2–3. (**D** and **E**). Phagocytic activity evidenced by ED-1 immunolabelling (green). (**F** and **G**). Expression of the class two major histocompatibility complex (MHC-II) (red) and rIL-1β (rat IL-1β–green) after AdIL-1ra treatment in 6-OHDA/LPS and Veh/LPS animals. (**F**) The SN of 6-OHDA/LPS + AdIL-1ra animals showed mostly stage 4 MHC-II+ cells. Ramified rIL-1β+cells were observed surrounding the lesion. (**G**) The SN of control animals exhibited a reduced number of MHC-II + and IL-1β+ cells at the injection site. Scale bar: 100 μm. B′, B″, C′, C″: Examples of different stages of microglial activation magnified from B and C (yellow circles): B′, Stage 3 amoeboid microglia with thick and stout processes; B″, Stage 4 phagocytic cell, round-shaped body; C′, Stage 2 rod-shaped cell and C″, Stage 3 amoeboid microglia. Scale bar B′, B″, C′, C″: 20 μm. (**H**) Quantitation of MHCII positive cells (stage 4) throughout the SN 21 days after 6-OHDA in animals with IL-1 activity inhibited (Ad IL-1ra – dark grey bars) or controls [Ad β-gal (light grey bars) or no Ad treatment (black bars)]. No statistically significant differences were found between the different treatments. (AdIL-1ra/6-OHDA/LPS $N = 3$, Ad β-gal/6-OHDA/LPS $N = 3$, AdIL-1ra/Veh/LPS $N = 3$, Ad β-gal/Veh/LPS $N = 3$). Error bars represent SEM.

or vehicle striatally lesioned rats at Day 7 post-lesion (Fig. 1). We chose this time point since we knew that IL-1 triggered inflammation in the periphery normally lasts for at least 5 days, impacting in the SN at similar time points (*ca*. 12 days post-6-OHDA) as in the other experimental set-ups (Fig. 1D). As a control for the systemic effects of AdIL-1, a total leucocyte count was made on blood samples taken five days after adenoviral injection but not on Day zero and compared to Ad β-gal injected animals (data not shown).

Interestingly, a statistically significant decrease in the number of TH-positive cells in the SN was observed in the animals treated with 6-OHDA/Ad IL1βiv in comparison with the other groups (Fig. 6A, $P<0.05$ 6-OHDA/Ad IL1βiv compared to 6-OHDA/Ad β-gal iv). No direct effect of systemic IL-1 was observed in animals with an intact SN (Veh/Ad IL-1 iv) suggesting that systemic IL-1 expression can exacerbate, but not directly elicit, neurodegeneration in the SN.

In addition, animals injected with 6-OHDA in the striatum and AdIL1β intravenously were the only ones to show stage 4 morphology by GSA-lectin staining (Fig. 6B) and ED1 immunoreactivity throughout the SN (Fig. 6C). A statistically significant difference in the amount of MHCII-positive cells was found between the 6-OHDA/Ad IL-1 iv group and the control groups (Fig. 6D, $P<0.01$).

IL-1 exacerbates neurodegeneration directly and via nitric oxide

To address the question of whether IL-1 is directly toxic to neurons, we used an *in vitro* cell culture model to exacerbate the effects of IL-1 observed previously *in vivo*. A human neuronal cell line was treated with 3.125 μM 6-OHDA and 1 day later, escalating non-toxic doses of IL-1 were added to the medium to see if this second treatment had any effect on the viability of the cells. The addition of IL-1 from 0.125 to 0.03 pg/μl had no effect *per se* on cell viability (percentage of viability 96.3% for 0.125 pg/μl, 97.5% for 0.0625 pg/μl, 95.54% for 0.05 pg/μl and 102.3% for 0.03 pg/μl, data not shown), but the three highest doses produced an exacerbating effect on 6-OHDA toxicity (Fig. 7A). Thus, we conclude that IL-1 is able to act directly on neurons and exacerbates 6-OHDA-triggered neuronal death.

We then investigated the role of other possible IL-1-induced molecules as possible mediators of IL-1 action. We studied the relevance of nitric oxide (NO) in this model by investigating iNOS expression and the appearance of nitrotyrosine (3-NT) immunoreactivity in the SN of 6-OHDA/LPS, 6-OHDA/Vehicle or Veh/LPS animals by immunohistochemistry. iNOS expression and 3-NT were detected almost exclusively on sections from 6-OHDA/LPS animals, suggesting a differential expression of NO in that group of animals (Fig. 7B and C).

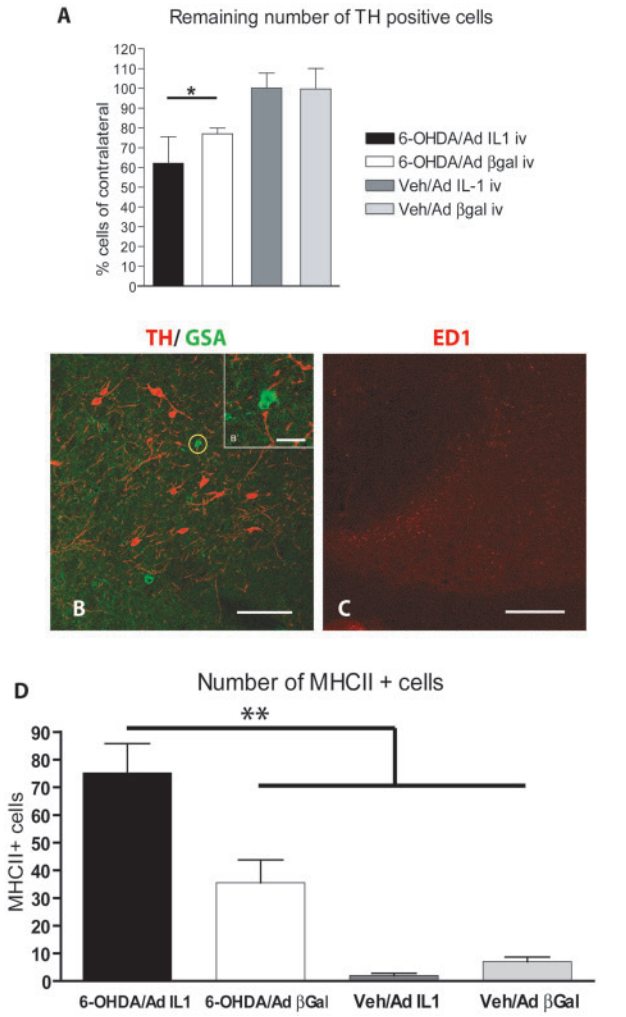

Fig. 6 Systemic Ad IL-1β injection increased neuronal loss in the SN. **(A)** Remaining number of TH-positive cells in the SN after systemic injection. Quantitation of TH-positive cells as a percentage of cells in the ipsilateral hemisphere versus the contralateral one. Two-way ANOVA (Striatum and systemic stimulus) with significant double interaction $P<0.05$ was followed by Fisher's LSD *post hoc* test. $^{*}P<0.05$, compare 6-OHDA/Ad IL-1βiv ($N=7$) to 6-OHDA/Ad β-gal iv ($N=6$). $N=9$ and 8 for Veh/Ad IL-1βiv and Veh/Ad β-gal iv groups, respectively). Error bars represent SEM. **(B** and **C)** Microglial activation in the SN of animals injected with 6-OHDA/Ad IL-1β i.v. B. GSA-positive (**B**) and ED-1-positive (**C**) cells at stage 4 were observed in the SN of 6-OHDA/AdIL-1β i.v. Scale bar B: 50 μm. Scale bar C: 100 μm. Inset in B (B'): magnification showing a stage 4 activated microglial cell. Scale bar inset (B'): 10 μm. (**D**) Quantitation of MHCII positive cells throughout the SN after systemic challenge. Two-way ANOVA (Striatum and systemic stimulus) with significant double interaction $P<0.01$ was followed by Fisher's LSD *post hoc* test. $^{**}P<0.01$ significant difference between 6-OHDA/Ad IL-1βiv compared to every other groups. $N=5$, 4, 5 and 5 for 6-OHDA/Ad IL-1βiv 6-OHDA/Ad β-gal iv, Veh/Ad IL-1βiv and Veh/Ad β-gal iv groups, respectively. Error bars represent SEM.

This result prompted us to test the functional relevance of this differential NO expression on dopaminergic cell loss in our experimental groups. Thus, 6-OHDA/LPS, 6-OHDA/Veh and Veh/LPS animals were treated i.p. with 10 mg/kg

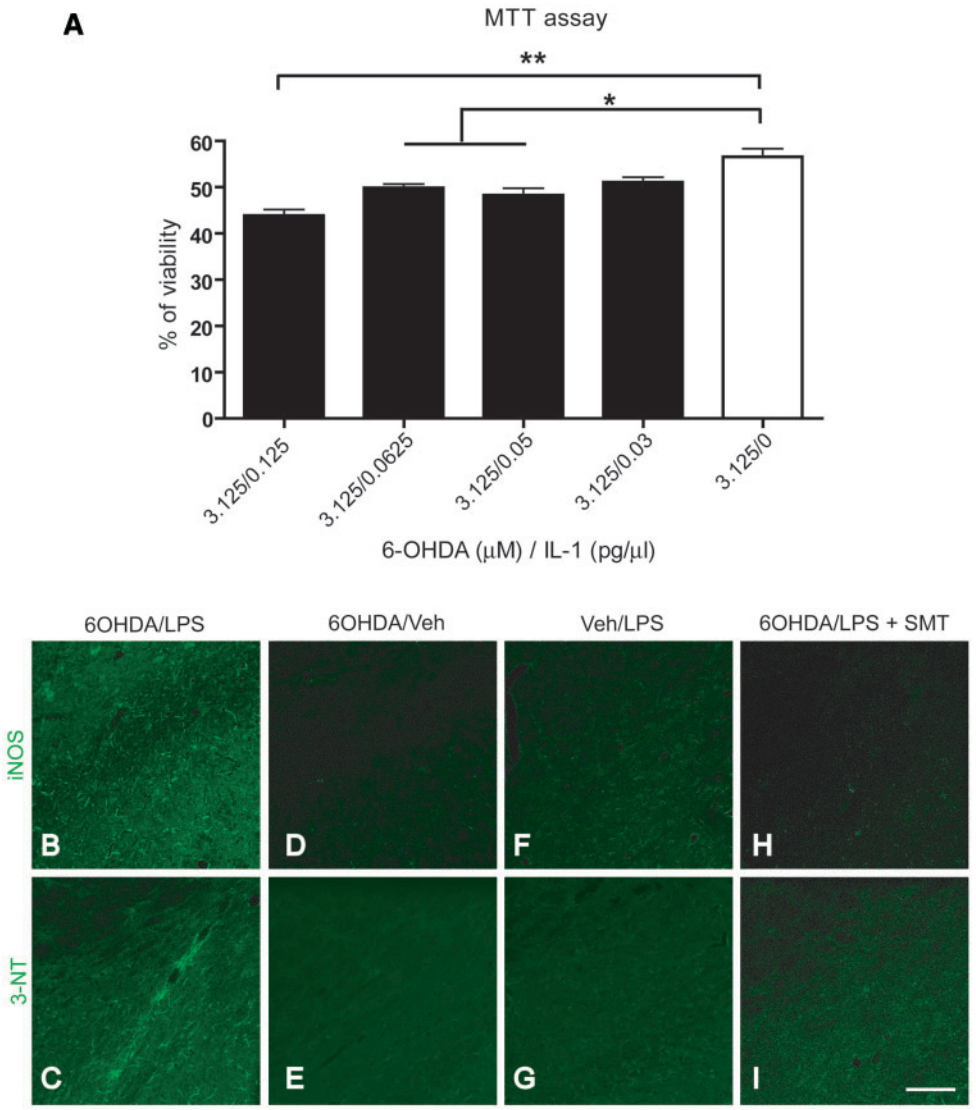

Fig. 7 **(A)** Viability of SK-N-SH cells tested by MTT assay. Cells were pre-treated with 6-OHDA and subjected to escalating doses of IL-1. Concentration-dependent decreases in cell viability in response to IL-1 were observed. One-way ANOVA followed by Fisher's LSD *post hoc* test. $^{**}P < 0.01$ significant difference between 3.125 μM 6-OHDA/0.0125 pg/μl of IL-1 and 3.125 μM 6-OHDA/0 pg/μl of IL-1. $^{*}P < 0.05$ significant difference between 3.125 μM 6-OHDA/0.0625 pg/μl of IL-1 or 3.125 μM 6-OHDA/0.05 pg/μl of IL-1 and 3.125 μM 6-OHDA/0 pg/μl of IL-1. Every group was normalized to 100%. Error bars represent SEM. **(B–I)** iNOS expression and 3-NT immunohistochemistry in different animal groups. (**B** and **C**). Ramified iNOS and 3-NT positive cells were observed within the SN of 6-OHDA/LPS-treated animals. (**D** and **E**) 6-OHDA/Veh animal group was completely devoid of iNOS and 3-NT immunoreactivity. (**F** and **G**) Veh/LPS animals exhibited a reduced immunoreactivity of ramified iNOS positive cells at the injection site. No 3-NT label was observed in this group. (**H** and **I**) No iNOS expression or 3-NT immunoreactivity was observed in the 6-OHDA/LPS+SMT-treated group. Scale bar: 100 μm.

of *S*-methylisothiourea (SMT) (Iravani *et al.*, 2002), a potent iNOS inhibitor, daily from the moment of the second stimulus (Day 12) till the day of sacrifice and TH-positive neurons were counted throughout the SN (Fig. 1). As expected, no expression of iNOS and 3-NT was found in the SMT-treated animals by immunohistochemistry (Fig. 7H and I). Only the 6-OHDA/LPS animals showed an increased number of TH-positive neurons in the SN after the SMT treatment, partially reversing the exacerbating effect of LPS (Fig. 2A). This inhibition of LPS action was not total since the values of TH-positive neurons in the 6-OHDA/LPS+SMT were significantly lower to the ones of the 6-OHDA/Veh + SMT group ($P < 0.05$) (Fig. 2A). These results suggest a main, but not exclusive participation of NO in the LPS exacerbating effect.

Then, we studied whether IL-1 expression was upstream of NO induction in our model of Parkinson's disease exacerbation. In order to address this issue, we studied whether the levels of IL-1 in the SN were affected by the inhibition of NO after the SMT treatment by ELISA. The changes in IL-1 levels were only marginally and not significantly altered by the SMT treatment in the 6-OHDA/LPS

group (see Fig. 4, $P = 0.176$ comparing 6-OHDA/LPS with and without SMT treatment), suggesting that NO production was downstream of IL-1 induction after the administration of LPS in the 6-OHDA animals.

In addition, to investigate the possible involvement of prostaglandins, we have studied the expression of cyclooxygenase-2 (COX-2) by RT-PCR on RNA samples from the SN of 6-OHDA/LPS, 6-OHDA/Veh- and Veh/LPS-treated animals. No differences in COX-2 expression were detected among the different experimental groups (data not shown).

Taking all these results together, we conclude that the most probable scenario is that IL-1 is acting both directly on neurons and indirectly via NO and possibly other unidentified molecules.

Discussion

In this study, we show for the first time that a sub-toxic dose of LPS injected in the degenerating SN exacerbates neuronal loss, shifts microglial activation to a pro-inflammatory phenotype, increases IL-1β production, and, importantly, produces earlier and increased motor disabilities compared to 6-OHDA-only treated animals. In addition, a common and widely used anti-inflammatory agent, DXM, was able to reverse the exacerbating effects of LPS. Furthermore, we demonstrate that IL-1 plays a major role in this exacerbation. Finally, chronic systemic expression of IL-1 was able to exacerbate neuronal demise and microglial activation in the SN, increasing the clinical impact of these findings. Evidence was found for direct and indirect effects of IL-1 on the exacerbation of 6-OHDA toxicity on dopaminergic neurons.

Inflammation can exacerbate neurodegeneration and motor symptoms in Parkinson's disease

Our results show that LPS can exacerbate neurodegeneration in the SN and aggravate and accelerate the appearance of behavioural symptoms in our Parkinson's disease model. Similar effects on neuronal loss were observed in animals where chronic, systemic inflammation was evoked. These results suggest that systemic or central inflammation could be regarded as a risk factor for the exacerbation of Parkinson's disease.

Inflammation has been ubiquitously found in the SN of animal models and Parkinson's disease patients. Infections such as influenza virus, Helicobacter pylori, HIV and even candidiasis and their accompanying inflammatory responses have also been suggested, but not proven, as etiological agents of Parkinson's disease (Arai *et al.*, 2006; Epp and Mravec, 2006). Specially, a case supporting the correlation between a major increase in parkinsonian symptoms and the influenza pandemic of 1918 has been widely discussed (Isgreen *et al.*, 1976; Ravenholt and Foege, 1982; Takahashi and Yamada, 1999; Marttila and Rinne, 1976). In light of our results that inflammation can accelerate the appearance of Parkinson's disease symptoms, it is possible to argue that infections can exacerbate an ongoing neurodegeneration in the SN of otherwise asymptomatic patients, rendering them symptomatic and thus, clinically defined as Parkinson's disease patients. On the other hand, the long-term expression of IL-1 in the periphery by adenoviral vectors did not cause overt neurodegeneration *per se*, indicating the need for a second event (i.e. an ongoing degeneration in the SN) to observe a toxic effect of systemic inflammation. Thus, although our data do not reject infections as etiological agents of Parkinson's disease, we favour the idea of inflammation as an exacerbating agent of Parkinson's disease.

Mechanisms of inflammation-triggered PD exacerbation

Whether microglial activation protects or exacerbates neuronal loss in the SN has been intensively debated (Vila *et al.*, 2001; Nagatsu, 2002; Hirsch *et al.*, 2003, 2005; Block and Hong, 2005; Hald and Lotharius, 2005; Kim and de Vellis, 2005). Microglial cells can be activated to different stages according to morphology, expressed markers and secreted products (Perry *et al.*, 2007). Morphological characteristics and cellular markers can be misleading in terms of the functional effect of activated microglia on neuronal demise (Perry *et al.*, 2007). In our study, stage 4 microglia and MHC II expression was associated with exacerbated neurodegeneration and motor symptoms. Whether this correlation is unique to our model or not, deserves future investigation. We confirmed the previously observed 'atypical' microglial activation during neurodegeneration in the SN in the 6-OHDA model (Depino *et al.*, 2003). This type of activation included transcription, but not translation, of major pro-inflammatory cytokines such as IL-1β and a stage 3, mostly ED-1-negative microglial phenotype. These observations correlate well with the biology of the chronic neurodegenerative model used: neuronal cell death in the SNpc is supposed to be apoptotic (He *et al.*, 2000), which by definition does not cause inflammation. Moreover, activated macrophages in the periphery do not express pro-inflammatory cytokines during phagocytosis of an apoptotic cell (Fadok *et al.*, 1998). In addition, microglial activation without pro-inflammatory cytokine production has also been observed in a model of prion disease (Perry *et al.*, 2002). Many treatments such as adherence of monocytes to a plastic surface can induce pro-inflammatory cytokine transcription uncoupled to translation in a variety of cells but the presence of an external pro-inflammatory agent such as LPS always elicits transcription 'and' translation of pro-inflammatory cytokines (Dinarello, 1991). We hypothesized that, in these microglial cells primed by the neurodegeneration caused by 6-OHDA where pro-inflammatory mRNAs are increased, but are not translated, a sub-toxic dose of

LPS could activate the translation of these already increased pro-inflammatory cytokine mRNAs. In turn, these increased, translated pro-inflammatory cytokines could shift the environment to a pro-inflammatory milieu, causing a toxic effect directly or by for example, the generation of NO and free radicals. All our data support this hypothesis. Results obtained by ELISA showed increased levels of IL-1 only in the 6-OHDA/LPS animals and the inhibition of this cytokine by the inoculation of AdIL-1ra or DXM could reverse the exacerbating effect. Sub-toxic levels of IL-1 were able to exacerbate 6-OHDA toxicity *per se* or by inducing other molecules such as NO. Interestingly, IL-1 inhibition had no effect on microglial activation, indicating that IL-1 production was a downstream event after microglial activation. In addition, NO inhibition did not significantly alter IL-1 production, suggesting that IL-1 induction is an upstream event from NO production.

These results support the emerging view that a second, pro-inflammatory stimulus on a region already under degeneration, can trigger increased IL-1 production and shift the equilibrium towards increased neurodegeneration. Indeed, Cunningham *et al*. (2005) have recently found that IL-1 could exacerbate disease symptoms in a prion disease model. Koprich *et al*. (2008) demonstrate that prior exposure to LPS renders animals more susceptible to a sub-toxic dose of 6-OHDA. Importantly, in their 'mirror image' approach, IL-1 blockage also leads to an amelioration of the toxic effects observed, reinforcing the notion that IL-1 is a key component of the inflammatory response that leads to Parkinson's disease onset or exacerbation.

In the present study, DXM treatment was also able to prevent inflammation-induced exacerbation of neuronal loss. From previous studies, other inflammatory mediators such as COX-2, free radicals, and nitric oxide have been proposed as targets of anti-Parkinson's disease therapies. (Hirsch and Hunot, 2000; Vila *et al*., 2001; Sanchez-Pernaute *et al*., 2004). Indeed, the use of minocycline, an antibiotic with anti-inflammatory and anti-apoptotic properties is being tested in a Phase III clinical trial for PD (NINDS-NET-PD-Investigators, 2006). In addition, an epidemiological study has associated the chronic use of ibuprofen with a 0.62–0.73 reduced risk of Parkinson's disease (Chen *et al*., 2005).

Our work identifies for the first time a clinically relevant animal model where inflammation is unequivocally detrimental to the SN. The major clinical impact we suggest is that central or systemic inflammation should be considered a risk factor for Parkinson's disease and should be efficiently handled or prevented in Parkinson's disease patients to reduce exacerbated disease progression. The identification of other molecular inflammatory targets and the extension of the present observations using additional systemic inflammatory models should help in defining the best therapeutic option for the prevention or inhibition of the exacerbating effects of inflammation in Parkinson's disease patients.

Acknowledgements

The authors wish to thank Profs. V. Hugh Perry and Daniel Anthony for their critical reading and suggestions on the manuscript and Mrs María Isabel Farías and Mr Fabio Fraga for their excellent technical assistance. This work was financially supported by the Michael J. Fox Foundation for Parkinson Research (FP), the Barón Foundation (FP) and the ANPCyT (FP). CF and FP are members of the research career of CONICET. MCPG is an YPF Foundation scholar and RT has a scholarship from the Fiorini Foundation.

References

Arai H, Furuya T, Mizuno Y, Mochizuki H. Inflammation and infection in Parkinson's disease. Histol Histopathol 2006; 21: 673–8.

Battista D, Ferrari C, Gage F, Pitossi F. Neurogenic niche modulation by activated microglia: transforming growth factor beta increases neurogenesis in the adult dentate gyrus. Eur J Neurosci 2006; 23: 83–93.

Besedovsky H, del Rey A. Immune-neuro-endocrine interactions: facts and hypotheses. Endocrin Rev 1996; 17: 1–39.

Block ML, Hong JS. Microglia and inflammation-mediated neurodegeneration: multiple triggers with a common mechanism. Prog Neurobiol 2005; 76: 77–98.

Chen H, Jacobs E, Schwarzschild MA, McCullough ML, Calle EE, Thun MJ, et al. Nonsteroidal antiinflammatory drug use and the risk for Parkinson's disease. Ann Neurol 2005; 58: 963–7.

Cunningham C, Wilcockson DC, Campion S, Lunnon K, Perry VH. Central and systemic endotoxin challenges exacerbate the local inflammatory response and increase neuronal death during chronic neurodegeneration. J Neurosci 2005; 25: 9275–84.

Delgado M, Ganea D. Neuroprotective effect of vasoactive intestinal peptive (VIP) in a mouse model of Parkinson's disease by blocking microglial activation. FASEB J 2003; 17: 944–6.

Depino AM, Alonso M, Ferrari C, del Rey A, Anthony D, Besedovsky H, et al. Learning modulation by endogenous hippocampal IL-1: blockade of endogenous IL-1 facilitates memory formation. Hippocampus 2004; 14: 526–35.

Depino A, Earl C, Kaczmarczyk E, Ferrari C, Besedovsky H, del Rey A, et al. Microglial activation with atypical pro-inflammatory cytokine expression in a rat model of Parkinson's disease. Eur J Neurosci 2003; 18: 2731–42.

Dinarello CA. Interleukin-1 and interleukin-1 antagonism. Blood 1991; 77: 1627–52.

Epp LM, Mravec B. Chronic polysystemic candidiasis as a possible contributor to onset of idiopathic Parkinson's disease. Bratisl Lek Listy 2006; 107: 227–30.

Fadok V, Bratton D, Konowal A, Freed P, Westcott J, Henson P. Macrophages that have ingested apoptotic cells in vitro inhibit proinflammatory cytokine production through autocrine/paracrine mechanisms involving TGF-b, PGE2, and PAF. J Clin Invest 1998; 101: 890–8.

Ferrari CC, Depino AM, Prada F, Muraro N, Campbell S, Podhajcer O, et al. Reversible demyelination, blood-brain barrier breakdown, and pronounced neutrophil recruitment induced by chronic IL-1 expression in the brain. Am J Pathol 2004; 165: 1827–37.

Ferrari CC, Pott Godoy MC, Tarelli R, Chertoff M, Depino AM, Pitossi FJ. Progressive neurodegeneration and motor disabilities induced by chronic expression of IL-1beta in the substantia nigra. Neurobiol Dis 2006; 24: 183–93.

Gao HM, Jiang J, Wilson B, Zhang W, Hong JS, Liu B. Microglial activation-mediated delayed and progressive degeneration of rat nigral dopaminergic neurons: relevance to Parkinson's disease. J Neurochem 2002; 81: 1285–97.

Hald A, Lotharius J. Oxidative stress and inflammation in Parkinson's disease: is there a causal link? Exp Neurol 2005; 193: 279–90.

He Y, Lee T, Leong S. 6-Hydroxydopamine induced apoptosis of dopaminergic cells in the rat substantia nigra. Brain Res 2000; 858: 163–6.

Hirsch EC, Breidert T, Rousselet E, Hunot S, Hartmann A, Michel PP. The role of glial reaction and inflammation in Parkinson's disease. Ann NY Acad Sci 2003; 991: 214–28.

Hirsch EC, Hunot S. Nitric oxide, glial cells and neuronal degeneration in parkinsonism. Trends Pharmacol Sci 2000; 21: 163–5.

Hirsch EC, Hunot S, Hartmann A. Neuroinflammatory processes in Parkinson's disease. Parkinsonism Relat Disord 2005; 11 (Suppl 1): S9–15.

Hunot S, Dugas N, Faucheux B, Hartmann A, Tardieu M, Debre P, et al. FcepsilonRII/CD23 is expressed in Parkinson's disease and induces, in vitro, production of nitric oxide and tumor necrosis factor-alpha in glial cells. J Neurosci 1999; 19: 3440–7.

Iravani MM, Kashefi K, Mander P, Rose S, Jenner P. Involvement of inducible nitric oxide synthase in inflammation-induced dopaminergic neurodegeneration. Neuroscience 2002; 110: 49–58.

Isgreen WP, Chutorian AM, Fahn S. Sequential parkinsonism and chorea following 'mild' inluenza. Trans Am Neurol Assoc 1976; 101: 56–60.

Kaur C, Ling E. Study of the transformation of amoeboid microglia cells into microglia labelled with the isolectin Griffonia simplicifolia in postnatal rats. Acta Anatomica 1991; 142: 118–25.

Kiefer R, Kreutzberg GW. Effects of dexamethasone on microglial activation in vivo: selective downregulation of major histocompatibility complex class II expression in regenerating facial nucleus. J Neuroimmunol 1991; 34: 99–108.

Kim SU, de Vellis J. Microglia in health and disease. J Neurosci Res 2005; 81: 302–13.

Kolb M, Margetts PJ, Anthony DC, Pitossi F, Gauldie J. Transient expression of IL-1beta induces acute lung injury and chronic repair leading to pulmonary fibrosis. J Clin Invest 2001; 107: 1529–36.

Koprich JB, Reske-Nielsen C, Mithal P, Isacson O. Neuroinflammation mediated by IL-1 beta increases susceptibility of dopamine neurons to degeneration in an animal model of Parkinson's disease. J Neuroinflammation 2008; 5: 8.

Kreutzberg GW. Microglia: a sensor for pathological events in the CNS. Trends Neurosci 1996; 19: 312–8.

Marttila RJ, Rinne UK. Arteriosclerosis, heredity, and some previous infections in the etiology of Parkinson's disease. A case-control study. Clin Neurol Neurosurg 1976; 79: 46–56.

McColl BW, Rothwell NJ, Allan SM. Systemic inflammatory stimulus potentiates the acute phase and CXC chemokine responses to experimental stroke and exacerbates brain damage via interleukin-1- and neutrophil-dependent mechanisms. J Neurosci 2007; 27: 4403–12.

McGeer PL, Itagaki S, McGeer EG. Expression of the histocompatibility glycoprotein HLA-DR in neurological disease. Acta Neuropathol 1988; 76: 550–7.

McGeer PL, McGeer EG. Inflammation and neurodegeneration in Parkinson's disease. Parkinsonism Relat Disord 2004; 10 (Suppl 1): S3–7.

Mirza B, Hadberg H, Thomsen P, Moos T. The absence of reactive astrocytosis is indicative of a unique inflammatory process in Parkinson's disease. Neuroscience 2000; 95: 425–32.

Nagatsu T. Parkinson's disease: changes in apoptosis-related factors suggesting possible gene therapy. J Neural Transmission 2002; 109: 731–45.

NINDS-NET-PD-Investigators.A randomized, double-blind, futility clinical trial of creatine and minocycline in early Parkinson disease. Neurology 2006; 66 (5): 664–71.

Olsson M, Nikkhah G, Bentlage C, Björklund A. Forelimb akinesia in the rat Parkinson model: Differential effects of dopamine agonists and nigral transplants as assessed by a new stepping test. J Neurosci 1995; 15: 3863–75.

Paxinos G, Watson C. The rat brain in stereotaxic coordinates. Orlando, FL: Academic Press; 1986.

Perry V, Cunningham C, Boche D. Atypical inflammation in the central nervous system in prion disease. Curr Opin Neurol 2002; 15: 349–54.

Perry VH, Cunningham C, Holmes C. Systemic infections and inflammation affect chronic neurodegeneration. Nat Rev Immunol 2007; 7: 161–7.

Pitossi F, del Rey A, Kabiersch A, Besedovsky H. Induction of cytokine transcripts in the central nervous system and pituitary following peripheral administration of endotoxin to mice. J Neurosci Res 1997; 48: 287–98.

Ravenholt RT, Foege WH. 1918 influenza, encephalitis lethargica, parkinsonism. Lancet 1982; 2: 860–4.

Sanchez-Pernaute R, Ferree A, Cooper O, Yu M, Brownell AL, Isacson O. Selective COX-2 inhibition prevents progressive dopamine neuron degeneration in a rat model of Parkinson's disease. J Neuroinflammation 2004; 1: 6.

Sauer H, Oertel WH. Progressive degeneration of nigrostrital dopamine neurons following intrastriatal terminal lesions with 6-OH dopamine: a combined retrograde tracing and immunocytochemical study in the rat. Neuroscience 1994; 59: 401–15.

Schallert T, Jones TA. 'Exuberant' neuronal growth after brain damage in adult rats: the essential role of behavioral experience. J Neural Transplant Plast 1993; 4: 193–8.

Takahashi M, Yamada T. Viral etiology for Parkinson's disease–a possible role of influenza A virus infection. Jpn J Infect Dis 1999; 52: 89–98.

Vila M, Jackson-Lewis V, Guégan C, Wu D, Teismann P, Choi D-K, et al. The role of glial cells in PArkinson's disease. Curr Opin Neurol 2001; 14: 483–9.

Wu DC, Jackson-Lewis V, Vila M, Tieu K, Teismann P, Vadseth C, et al. Blockade of microglial activation is neuroprotective in the 1-methyl-4-phenyl-1,2,3,6-tetrahydropyridine mouse model of Parkinson disease. J Neurosci 2002; 22: 1763–71.